Scientific Research Publishing

Advances in Materials Physics and Chemistry, 2017, 7, 334-346
http://www.scirp.org/journal/ampc
ISSN Online: 2162-5328
ISSN Print: 2162-531X

Description of New Bioelectromechanical Properties in Alginate: An Insight with a Computer Simulation

A. Heredia[1*], J. J. Gervacio-Arciniega[2], V. Duarte-Alaniz[3], O. Amelines-Sarria[4,5], A. Rodríguez-Galván[1], J. M. Siqueiros[2]

[1]Instituto de Ciencias Nucleares, Departamento de Química de Radiaciones y Radioquímica, Universidad Nacional Autónoma de México, Ciudad de México, Mexico
[2]Facultad de Ciencias Físico-Matemáticas, Benemérita Universidad Autónoma de Puebla, Puebla, México
[3]Instituto de Química, Universidad Nacional Autónoma de México, Ciudad de México, México
[4]Centro de Investigación y Desarrollo Tecnológico en Energías Renovables, Universidad de Ciencias y Artes de Chiapas, Tuxtla Gutiérrez, México
[5]Facultad de Ingeniería Mecánica, Universidad Pontificia Bolivariana Seccional Bucaramanga, Floridablanca, Colombia

Email: *aheredia@nucleares.unam.mx

How to cite this paper: Heredia, A., Gervacio-Arciniega, J.J., Duarte-Alaniz, V., Amelines-Sarria, O., Rodríguez-Galván, A. and Siqueiros, J.M. (2017) Description of New Bioelectromechanical Properties in Alginate: An Insight with a Computer Simulation. *Advances in Materials Physics and Chemistry*, **7**, 334-346.
https://doi.org/10.4236/ampc.2017.78026

Received: July 6, 2017
Accepted: August 14, 2017
Published: August 17, 2017

Abstract

Alginate biopolymer from *Tropicalgin C*302245 was studied by means of piezoresponse force microscopy imaging, scanning electron microscopy, powder X-rays, infrared spectroscopy and computer simulations. Local piezoresponse force microscopy images show possible ferroelectric domains detected in the out of plane mode and these results are confirmed by the second harmonic generation analysis. Alginate powder is composed by diatom frustules containing a cristobalite-like compound, amorphous silica and chitin. The experimental results are explained by *MM*+ and *PM*3 computer simulations that establish that the self-assembly of the alginate molecules enhance the polarization increasing the molecular collective dipole moment. Alginate molecular properties might open interesting possibilities for organic technological applications.

Keywords

Alginate, Piezoresponse Force Microscopy, Ferroelectricity, Macromolecular Self-Assembly

1. Introduction

In living matter, electricity plays a main role in signaling and other molecular-

related functions as stated by Galvani and Volta [1]. Voltage-gated signaling [2] is found in a wide distribution of taxa, from bacterial biofilms [3], plant tonoplasts [4] up to mammal neurons [5], thus the relevance of the energy from potentials and moving electrons must be a prerequisite for cellular response. At the molecular scale, electric potentials might stimulate changes in the conformational features of peptides [6] and in the classic experiments of the synthesis of amino acids [7] electric potential was of main relevance. The Mexican scientist Alfonso Luis Herrera noting the importance of the electricity in molecules, stated "(...) Nevertheless, the modern and fertile ideas about the ionization of molecules tend to give prominence to the production of physico-chemical phenomena by direct or indirect, mediate or intermediate electric forces and actions. The true philosopher is always ready to believe these transformations of energy and the true naturalist expects and provides the constant transformation of species" [8]. Other works analyze the main role of bioferroelectricity in molecular order and functionality of biological membrane channels [9] [10]. Many biologically-originated materials possess piezoelectric properties at the nanoscale [11] such aspolymers, biomolecules and bio-structures already published [12] [13] [14] [15] [16]. It seems that molecular ferroelectricity is relevant in biology [9] [14] [17] [18] [19] thus, rising an enquiry: whether or not the biomolecular electrical properties are relevant in biological activity, coordinating an additional molecular selection and self-assembly? If so, that assumption might contribute to the understanding of the biological functionality [20]. Piezoelectricity was discovered on wood by Shubnikov in 1946, and afterwards in other organisms tissues (teeth, horns, and cartilages) [21] and soft tissues (human pineal gland [22]), as well as on the micro and nanoscopic scales by using the piezoresponse force microscopy (PFM) [23]. The piezoresponse force microscopy is the most descriptive method to get insight into the piezoelectric and ferroelectric phenomena at the nanoscale [23] in different materials. Nevertheless, the comprehension of these phenomena at the molecule scale has not been explained accurately, more specifically, why polymers present this effect [24].

Alginatesas biopolymers in bacteria seem to play a structural function, affording mechanical strength and flexibility, meanwhile the molecule grasps water [25]. Alginates are polymers of two alternating acidic monomers, α-L-guluronic (G) and β-D-mannuronic (M) organized in different oligomers rich in G units and blocks rich in M units. The mechanical properties of alginates depend on the G: M ratio and has a relatively easy industrial production [26]. For this reason, and its biocompatibility, alginate has emerged as biologically relevant hydrogel material for drug delivery [27]. In other studies, alginate is used in inkjettechnology to produce three dimensional assemblies mediated by different voltages [28] [29] what makes us to consider the feasibility to possess some electromechanical features. Hence, it is a necessity to get an insight into the activity of the alginate under the electric field at the molecular-scale. Here, we report, the potential nanoscale bioferroelectricity in the biopolymer alginate (**Figure 1**). In biological self-assembled macromolecules, it is possible that different molecule-

scale mechanisms activate ferroelectric memory effects [30] [31] [32]. These properties will be useful to design green computer memories, biosensors and harvest energy devices [30]. The observed promising ferroelectric behavior adds a new important functionality to this well-known biomaterial.

2. Materials and Methods

The samples were the Alginate single dose *Tropicalgin C*302245, (lot 150884, Zhermack Clinical, Rome, Italy) commercially obtained. Directly from the package, the samples were used with no further treatment.

2.1. Scanning Electron Microscopy (SEM)

All the samples were fixed in a sample holder using only carbon ribbon, without any additional preparation. Scanning electron microscopy (ultra high resolution JSM-7800 FS chottky Field Emission Scanning Electron Microscope) instrument was used. We performed the measurements in a vacuum of 0.55 MPa, with an acceleration voltage between 2 - 5 kV.

2.2. X-Ray Diffraction (XRD)

For the XRD study, powder samples were put in a Phillips X'pert instrument with a Cu-Kα1 radiation at room temperature. We performed the data collection using a step size of 0.5˚ over 10˚ - 80˚ 2θ range (**Figure 2**).

2.3. Attenuated Total Reflection-Fourier Transform Infrared Spectroscopy (ATR-FTIR)

Infrared spectra were performed in an ATR-FTIR instrument (Spectrum 100 FT-IR Spectrometer Perkin Elmer, Waltham, Massachusetts) from 4000 to 650 cm^{-1} scan (6 scans). A first inspection of the ATR-FTIR obtained data, showed the typical bands found for diatom biosilica [33] [34] (**Figure 3**).

2.4. Piezoresponse Force Microscopy (PFM)

Samples were cast and fixed with no further treatment to be visualized by the

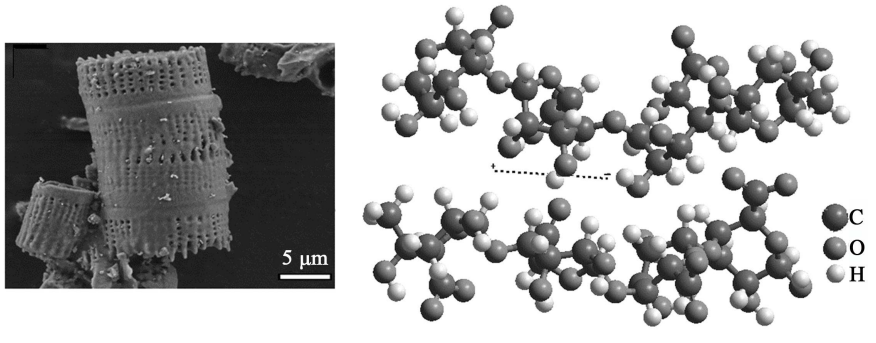

(a) (b)

Figure 1. (a) SEM microphotographs showing the morphology of the diatom from alginate powder *Tropicalgin C*302245 and (b) the molecular structure used for the computer simulations.

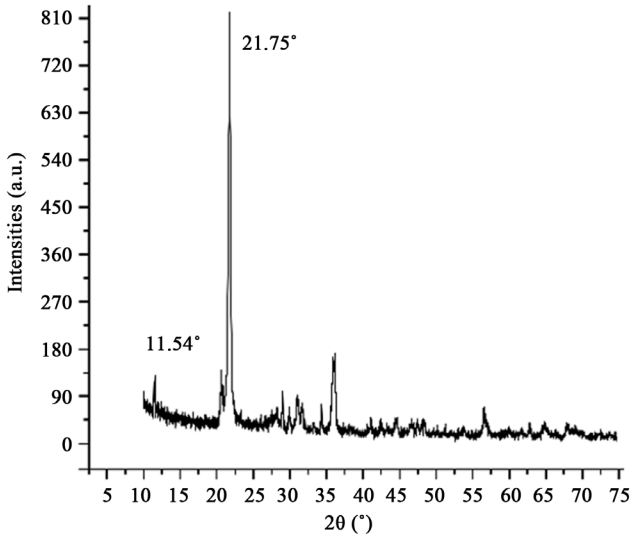

Figure 2. X-ray diffractogram of the alginate powder sample where the crystalline material and amorphous organic biopolymeric (background) phase are identified. The peak height reflects aqualitative increase in size of the biopolymer-associated crystallites.

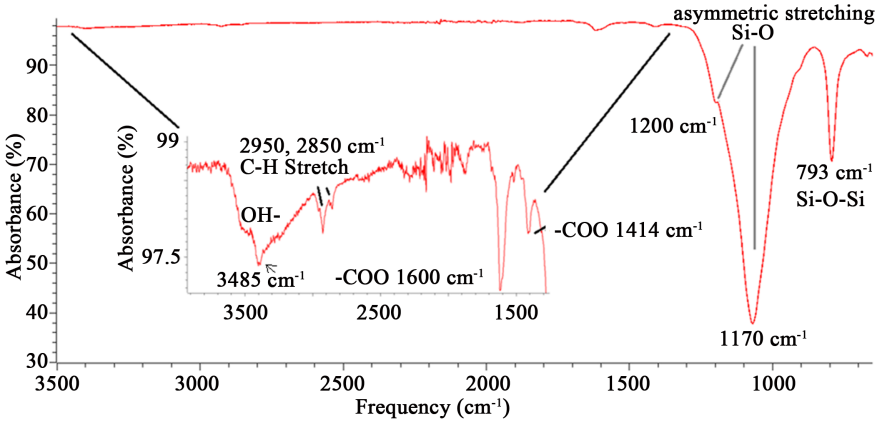

Figure 3. ATR-FTIR spectrum showing different bands corresponding to SiO_2 from biosilica, alginate and chitin.

atomic force microscopy (AFM) and PFM methods. The PFM technique detects the mechanical response of the sample to an applied electric voltage (electrostriction) due to the converse piezoelectric effect. Alginate was already studied in the AFM, by casting the samples from water solutions having stable surfaces [35]. In our work, here, after a first inspection, we performed the imaging in the areas with flat geometry.A commercial atomic force microscope (XE-70, Park Systems, Suwon, Korea) with a conductive *ElectricCont-G* cantilever from Budget Sensors (free resonance frequency 13 kHz, force constant 0.4 $N \cdot m^{-1}$) coupled with an external lock-in amplifier (SR865, Stanford Research Systems, USA) was used (**Figure 4**).

2.5. Molecular Simulations

HyperChem8.0.1. Molecular structures of β-D-mannuronate (M) and α-L-gu-

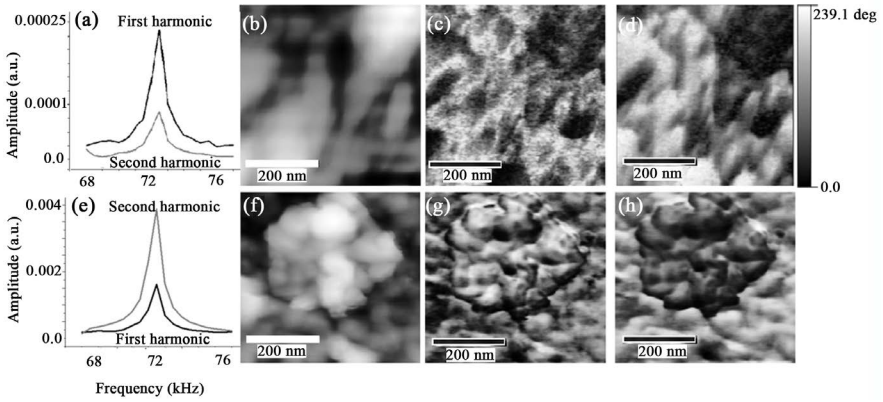

Figure 4. Second harmonic of the alginate sample ((a) and (e)). Atomic force microscopy tapping mode topography ((b), (f)) of a selected area of the *Tropicalgin C*302245 powder. ((c), (g)) Amplitude and ((d), (h)) Phase images. PFM signals ((c), (d), (g), (h)) in a selected area of the sample with a homogeneous topography exhibiting the blotched spatially resolved ferroelectric patterns ((c), (d)) appearing to be ferroelectric switched domains out of plane.

luronate (G) were created by using HyperChem8.0.1 and geometrically optimized for one up to 5 units (**Figures 5-7**). Further, the alginate (G-G-M-M units) was put together for self-assembly from two up to ten alginate chains (**Figure 5(c)** and **Figure 5(d)**). Molecular modeling MM+ was done with molecular mechanics and, afterwards, by semi-empirical quantum mechanics methods as implemented in the HyperChem program Version 8.0.1 (HyperCube, Canada). Geometry optimizations were used to obtain the optimized molecular coordinates at potential energy minima. Full geometry optimization of different alginate-forming monomers (β-D-mannuronate) and α-L-guluronate were performed by using the HyperChem settings in the MM+ force field (the Polak–Ribiere conjugate gradient algorithm, and a root mean square gradient (RMS) of 0.0001 kcal·Å^{-1}·mol^{-1}). Molecular dynamics relaxation of the optimized structures was employed to obtain to possible local minima (step size of 0.001 ps, a simulation temperature of 298 K and *ca.* 8 ps each model). The optimized geometries obtained by the MM+ molecular mechanics method were further optimized with the *PM3*. In semi-empirical calculations, full geometry optimizations were performed on the Restricted Hartree-Fock (RHF) basis (Polak-Ribiere conjugate gradient algorithm, and total RMS gradient of 0.001 kcal·Å^{-1}·mol^{-1} step size of 0.001 ps, constant simulation temperature of 298 K and *ca.* 3 ps each model).

GAMESS. The molecules were edited from HyperChem8.0.1 and afterwards in Avogadro 1.2.0 [36] and exported for GAMESS software [37]. We used the *PM3* semi-empirical calculations and a run type of Optimization with Restricted Hartree-Fock (RHF) molecule charge 0 and spin multiplicity 1.

3. Results and Discussion

Alginate (*Tropicalgin C*302245) powder is composed by diatom frustules (**Figure 1**) seeming to have a highly crystalline material (**Figure 2**) resembling

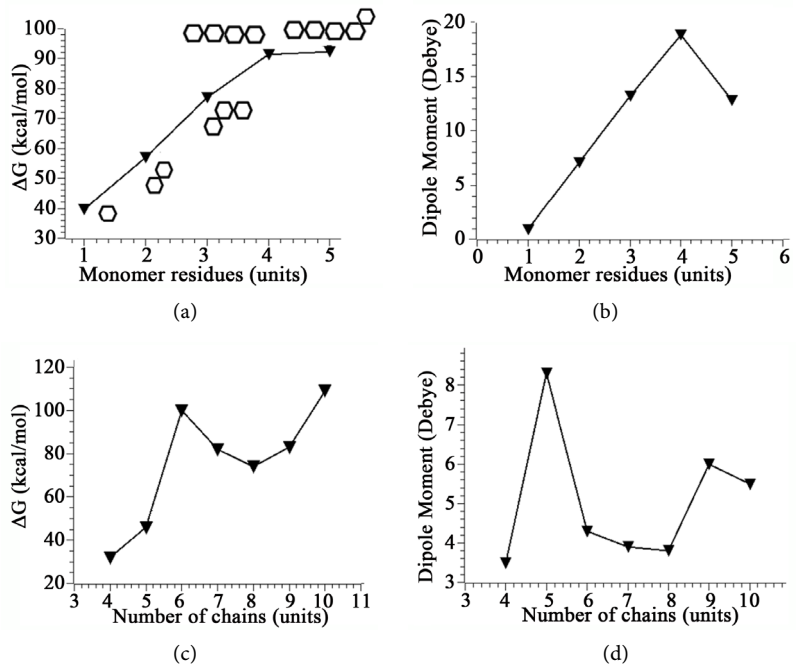

Figure 5. MM+ force field results show a loss in general stability values in the alginate molecules. A saturation region in the stability (in (a) at four to five units) through the augmentation of units is seen. In (b) an increase in the dipole moment is seen at the value of 4 units. The simulation of the assembly of different chains ((c), (d)) decreases the stability of the system such as in the increase single chain molecular mass ((a), (b)).

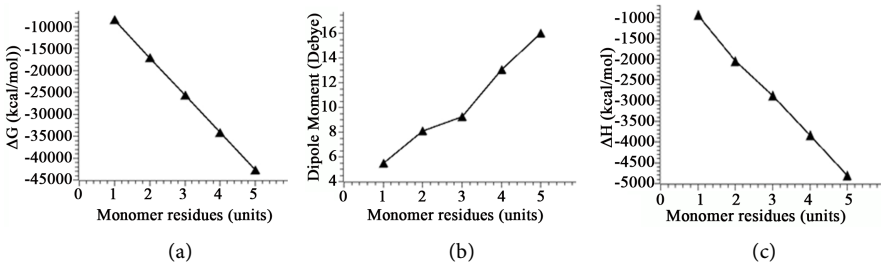

Figure 6. *PM3* semi-empirical results show an increasing stability (decreasing values) of energy in (a) in the growth of an alginate chain and an increase in the dipole moment (b) and a reduction in the heat formation.

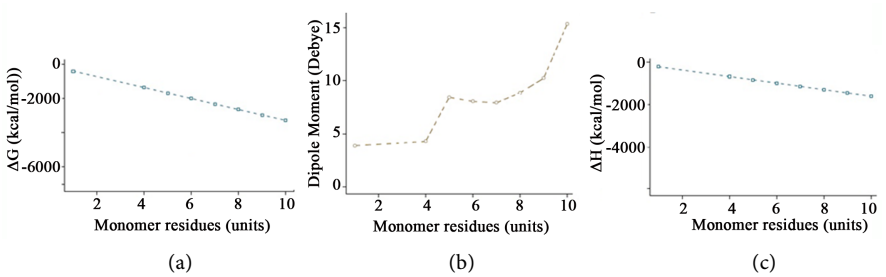

Figure 7. *PM3* semi-empirical resultsin GAMESS (dotted lines) show decreasing energy values (a) when increasing the monomer residues and an increase in the dipole moment (b) and a reduction in the heat formation values (c). These results contrast with the experimental values (lines).

other studies containing opal-cristobalite of fossil diatoms [38] [39]. X-ray structural parameters from alginate powder shows a very crystalline material corresponding tocristobalite crystalline solid (**Figure 2**). In the case the IR spectra, they show the characteristics set of SiO_2 bands from biosilica [33], alginate [40] [41] and chitin [42] [43]. Concretely, the band at 3437 cm^{-1} is due to the stretching vibration of -OH group and correspondingly, the IR band at *ca.*1617 cm^{-1} is due to the adsorbed water molecules. A strong and broad FTIR band at 1170 cm^{-1} with a shoulder close to 1200 cm^{-1} is usually assigned to the Si-O-Si asymmetric stretching vibrations, whereas the IR band at 793 cm^{-1} can be assigned to Si-O-Si symmetric stretching vibrations [44]. Alginate spectrum demonstrates the characteristic absorption bands of its polysaccharide structure (inset in **Figure 3**), symmetric 1414 cm^{-1} and asymmetric 1600 cm^{-1} (C–O stretching) from the carboxylate salt groups. Conversely, the bands at 1126 cm^{-1} (C–C stretching), 1021 cm^{-1} (C–O–C stretching) and 947 cm^{-1} (C–O stretching) are screened by the SiO_2 bands. The partially masked chitin bands at *ca.* 3250 cm^{-1}, (amide I) *ca.* 1650 cm^{-1} and amide II *ca.* 1550 cm^{-1} (in **Figure 3**, vertical gray lines in inset) confirms the presence of this molecule in diatom biosilica as described already [45].

The AFM allows for a non-destructive inspection of the surface of the sample and the direct monitoring of possible domain structures by means of PFM (**Figure 4(a)** and **Figure 4(b)**). This procedure allows studying the local properties such as polarization reversal. Piezoresponse force microscopy in the resonance mode was used to obtain evidence of the ferroelectric behavior of alginate (4B). To determine the amplitude of the AC voltage used in the PFM measurements, the first and second harmonics of the alginate sample were measured by the application of Vac = 1 Vpp over the sample. Clearly, the first harmonic is greater than the second one (**Figure 4(a)**). These results confirm that alginate might present ferroelectricity [46]. The piezoresponse images (**Figure 4(c)** and **Figure 4(d)**), were obtained by applying 1 Vpp at 71.5 kHz on a 500 nm by 500 nm square area. The PFM phase (**Figure 4(d)**) zones present similar topographical heights (**Figure 4(b)**) although exposing opposite polarization, defining that the observed contrast is due to the changing orientation of the dipole moments. These results agree with theoretical calculations shown later. However, by using Vac = 2 Vpp, displaying a clear topography (**Figure 4(F)**), the second harmonic is higher than the first one (see **Figure 4(e)**) thus, presenting no domain contrast in amplitude [47] [48] (**Figure 4(g)** and **Figure 4(h)**). The alginate dipolar direction might correlate to the internal rotation of the dipole moment-related chemical groups in asymmetric carbon atoms in the polysaccharide [48]. **Figure 4**, shows the poled sample with areas with different polar phases that are distributed randomly along the alginate sample. The switching contrast (**Figure 4(c)** and **Figure 4(g)**) does not follow directly the topographic aspect, indicating that the rearrange effect might be due to the intrinsic ferroelectric properties of the alginate and not induced from the surface electrostatic effects. Our result agrees with other biopolymers [49].

The computational molecular modeling of the different alginate units was performed to understand, at the molecular scale, the effects of the self-assembly on the dipole moments. An isolated monomer was optimized, and subsequently covalently linked to other monomers (up to 5 in **Figure 5(a)** and **Figure 5(b)**). The next procedure was to put to interact the 4 up to 10 molecules (**Figure 5(c)** and **Figure 5(d)**). Here, the models were studied by the geometry optimization of the total energy, and molecular dynamics cycles run using molecular mechanics (MM+) method in combination with a *semi-empirical* method PM3 (in RHF).

MM+ computer simulations show in **Figure 5(a)** and **Figure 5(c)**, a reduction global stability values, contrasting with those from *PM3* in HyperChem and GAMESS software, suggesting an increase in the thermodynamic stability. Alginate units in MM+ molecular simulations show an increment in the molecular dipole moment values when increasing the molecular mass of the chain up to 4 units and after wards a loss in dipole moment values are seen (**Figure 5(b)** and **Figure 5(d)**). In contrast, *PM3* semi-empirical method in HyperChem, partially agrees with the MM+ in the enhancement of the dipole moment values when increasing the molecular size of the chain (**Figure 5(b)**) thus, making suitable that the increase in the alginate single chains molecular size, rises the flexibility of the molecules, yielding higher dipole moment values (**Figure 6**). *PM3* semi-empirical simulation of alginate chain growth in GAMESS software, results in similar behavior to those obtained by HyperChem software although with different values. The most similar ones are the dipole moments in both software (**Figure 6** and **Figure 7**).

PM3 semi-empirical values of the assemblies of different number of alginate chains (not shown) show increasing positive energy (loss in general stability and in the ΔH) what agrees with the fact that alginate molecules stabilize through the interaction with inorganic ions [50] [51] and other organic compounds [52]. This precedent allows us to further simulate in the future, the self-assembly of alginate chains, considering those stabilizing ions and molecules.

4. Conclusion

The alginate powder presents a clear content with different diatom species, together with the molecular assembly (**Figures 1-3**). The molecular structure resembles the SiO_2 biosilica with features of a crystalline cristobalite-like solid (**Figure 2** and **Figure 3**). Regarding the PFM imaging and switching behavior, our findings suggest that alginate presents a ferroelectric effect and an efficient optical second harmonic generation. The biophysical purpose or aim of this organic-inorganic ferroelectric component is far away from our study, although brings a possible molecular transducer and biocontrol for detection of local electrostatic charges. This kind of polymer can be easily applied in different bionanotechnological instruments developing electromechanical biocompatible systems. The direct measurements of the spontaneous polarization with the PFM in

alginate are still necessary to understand its molecular origin. Nonetheless MM+ computer simulations bind together the increase of the molecular size of the polysaccharide and the variation of the energy values, electric dipole moment properties and of ΔH that further behaves such as contingent properties (**Figures 5-7**) in HyperChem and GAMESS software. The coordination of the genetic code to produce different molecular weights makes more elaborated to conclude the structural relationship between the dipole moments and the electromechanical behavior. Our preliminary results will be useful to attempt to understand these phenomena, mainly alginate self-assembly and the rising of the bioferroelectric effect.

Acknowledgements

Bach. InChem. Claudia Consuelo Camargo Raya (at ICN, UNAM) and Bach. Biol. Isabel Mejía Luna (At Departamento de física, Facultad de Ciencias, UNAM), (AH) to PAPIIT Project IA203616 and (AH) to Dirección General de Cómputo y de Tecnologías de Información y Comunicación (DGTIC) for Miztli facility through the Project SC16-1-IR-93. We also thank to Luciano Díaz González, Martín Cruz Villafañe, Luis Miguel Valdez Pérez, Ing. Juan Eduardo Murrieta León, Mat. Enrique Palacios Boneta and Phys. Antonio Ramírez Fernández for their technical assistance.

References

[1] De Micheli, A. (2011) En torno a los primeros estudios de electrofisiología. *Archivos De Cardiologia De Mexico*, **81**, 337-342.

[2] Hodgkin, A.L. and Huxley, A.F. (1952) A Quantitative Description of Membrane Current and Its Application to Conduction and Excitation in Nerve. *The Journal of Physiology*, **117**, 500-544. https://doi.org/10.1113/jphysiol.1952.sp004764

[3] Prindle, A., Liu, J., Asally, M., Ly, S., Garcia-Ojalvo, J. and Süel, G.M. (2015) Ion Channels Enable Electrical Communication in Bacterial Communities, *Nature*, **527**, 59-63. https://doi.org/10.1038/nature15709

[4] Bonales-Alatorre, E., Shabala, S., Chen, Z.-H. and Pottosin, I. (2013) Reduced Tonoplast Fast-Activating and Slow-Activating Channel Activity Is Essential for Conferring Salinity Tolerance in a Facultative Halophyte, Quinoa. *Plant Physiology*, **162**, 940-952. https://doi.org/10.1104/pp.113.216572

[5] Bean, B.P. (2007) The Action Potential in Mammalian Central Neurons. *Nature Reviews Neuroscience*, **8**, 451-465. https://doi.org/10.1038/nrn2148

[6] Chen, Y., Cruz-Chu, E.R., Woodard, J., Gartia, M.R., Schulten, K. and Liu, L. (2012) Electrically Induced Conformational Change of Peptides on Metallic Nano-Surfaces. *ACS Nano*, **6**, 8847-8856. https://doi.org/10.1021/nn3027408

[7] Lazcano, A. and Bada, J.L. (2003) The 1953 Stanley L. Miller Experiment: Fifty Years of Prebiotic Organic Chemistry. *Origins of Life and Evolution of Biospheres*, **33**, 235-242. https://doi.org/10.1023/A:1024807125069

[8] Cleaves, H.J., Lazcano, A., Ledesma Mateos, I., Negrón-Mendoza, A., Peretó, J. and Silva, E. (2014) Herrera's "Plasmogenia" and Other Collected Works Early Writings on the Experimental Study of the Origin of Life.

[9] Leuchtag, H.R. (1987) Indications of the Existence of Ferroelectric Units in Excita-

ble-Membrane Channels. *Journal of Theoretical Biology*, **127**, 321-340. https://doi.org/10.1016/S0022-5193(87)80110-8

[10] Bystrov, V.S. and Leuchtag, H.R. (1994) Bioferroelectricity: Modeling the Transitions of the Sodium Channel. *Ferroelectrics*, **155**, 19-24. https://doi.org/10.1080/00150199408007477

[11] Wojnar, R. (2012) Piezoelectric Phenomena in Biological Tissues. In: Ciofani, G. and Menciassi, A., Eds., *Piezoelectric Nanomater*, Biomedical Applications, Springer, Berlin Heidelberg, 173-185. https://doi.org/10.1007/978-3-642-28044-3_6

[12] Kalinin, S.V., Rodriguez, B.J., Shin, J., Jesse, S., Grichko, V., Thundat, T., Baddorf, A.P. and Gruverman, A. (2006) Bioelectromechanical Imaging by Scanning Probe Microscopy: Galvani's Experiment at the Nanoscale. *Ultramicroscopy*, **106**, 334-340. https://doi.org/10.1016/j.ultramic.2005.10.005

[13] Güthner, P. and Dransfeld, K. (1992) Local Poling of Ferroelectric Polymers by Scanning Force Microscopy. *Applied Physics Letters*, **61**, 1137-1139. https://doi.org/10.1063/1.107693

[14] Heredia, A., Meunier, V., Bdikin, I.K., Gracio, J., Balke, N., Jesse, S., Tselev, A., Agarwal, P.K., Sumpter, B.G., Kalinin, S.V. and Kholkin, A.L. (2012) Nanoscale Ferroelectricity in Crystalline γ-Glycine. *Advanced Functional Materials*, **22**, 2996-3003. https://doi.org/10.1002/adfm.201103011

[15] Kolosov, O., Gruverman, A., Hatano, J., Takahashi, K. and Tokumoto, H. (1995) Nanoscale Visualization and Control of Ferroelectric Domains by Atomic Force Microscopy. *Physical Review Letters*, **74**, 4309-4312. https://doi.org/10.1103/PhysRevLett.74.4309

[16] Gruverman, A., Auciello, O. and Tokumoto, H. (2003) Imaging and Control of Domain Structures in Ferroelectric Thin Films via Scanning Force Microscopy. *Annual Review of Materials Science*, **28**, 101-123. http://www.annualreviews.org/doi/10.1146/annurev.matsci.28.1.101 https://doi.org/10.1146/annurev.matsci.28.1.101

[17] Li, J., Liu, Y., Zhang, Y., Cai, H.-L. and Xiong, R.-G. (2013) Molecular Ferroelectrics: Where Electronics Meet Biology. *Physical Chemistry Chemical Physics*, **15**, 20786-20796. https://doi.org/10.1039/c3cp52501e

[18] Shamos, M.H. and Lavine, L.S. (1967) Piezoelectricity as a Fundamental Property of Biological Tissues. *Nature*, **213**, 267-269. https://doi.org/10.1038/213267a0

[19] Amdursky, N., Beker, P., Schklovsky, J., Gazit, E. and Rosenman, G. (2010) Ferroelectric and Related Phenomena in Biological and Bioinspired Nanostructures. *Ferroelectrics*, **399**, 107-117. https://doi.org/10.1080/00150193.2010.489871

[20] Tesson, B. and Charrier, B. (2014) Brown Algal Morphogenesis: Atomic Force Microscopy as a Tool to Study the Role of Mechanical Forces. *Frontiers in Plant Science*, **5**, 471. https://doi.org/10.3389/fpls.2014.00471

[21] Ciofani, G. and Menciassi, A. (2012) Piezoelectric Nanomaterials for Biomedical Applications. Springer Science & Business Media, Berlin. https://doi.org/10.1007/978-3-642-28044-3

[22] Lang, S.B., Marino, A.A., Berkovic, G., Fowler, M. and Abreo, K.D. (1996) Piezoelectricity in the Human Pineal Gland. *Bioelectrochemistry and Bioenergetics*, **41**, 191-195. https://doi.org/10.1016/S0302-4598(96)05147-1

[23] Gruverman, A. and Kholkin, A. (2006) Nanoscale Ferroelectrics: Processing, Characterization and Future Trends. *Reports on Progress in Physics*, **69**, 2443-2474. https://doi.org/10.1088/0034-4885/69/8/R04

[24] Tuszynski, J.A., Craddock, T.J.A. and Carpenter, E.J. (2008) Bio-Ferroelectricity at the Nanoscale. *Journal of Computational and Theoretical Nanoscience*, **5**, 2022-2032. https://doi.org/10.1166/jctn.2008.1008

[25] Halverson, L.J. (2009) Role of Alginate in Bacterial Biofilms. In: Rehm, B.H.A., Ed., *Alginates*: *Biology and Applications*, Springer, Berlin Heidelberg, 135-151. https://doi.org/10.1007/978-3-540-92679-5_6

[26] Arvizu-Higuera, D.L., Hernández-Carmona, G. and Rodriguez-Montesinos, E. (1996) Effect of Temperature and Extraction Time on the Process to Obtain Sodium Alginate from Macrocystis Pyrifera. *Ciencias Marinas*, **22**, 511-521.

[27] Paradee, N., Sirivat, A., Niamlang, S. and Prissanaroon-Ouajai, W. (2012) Effects of Cross Linking Ratio, Model Drugs, and Electric Field Strength on Electrically Controlled Release for Alginate-Based Hydrogel. *Journal of Materials Science*: *Materials in Medicine*, **23**, 999-1010. https://doi.org/10.1007/s10856-012-4571-0

[28] García Herrera, C., Espinoza Matheus, N., Orellana Jaimes, N., Antonio Ramírez, R. and Setién Duín, V. (2008) Técnica de impresión con alginato: Una propuesta edumática. *Acta Odontológica Venez*, **46**, 180-183.

[29] Dohnal, J. and Štěpánek, F. (2010) Inkjet Fabrication and Characterization of Calcium Alginate Microcapsules. *Powder Technology*, **200**, 254-259. https://doi.org/10.1016/j.powtec.2010.02.032

[30] Tayi, A.S., Kaeser, A., Matsumoto, M., Aida, T. and Stupp, S.I. (2015) Supramolecular Ferroelectrics. *Nature Chemistry*, **7**, 281-294. https://doi.org/10.1038/nchem.2206

[31] Kalinin, S.V., Rodriguez, B.J., Jesse, S., Karapetian, E., Mirman, B., Eliseev, E.A. and Morozovska, A.N. (2007) Nanoscale Electromechanics of Ferroelectric and Biological Systems: A New Dimension in Scanning Probe Microscopy. *Annual Review of Materials Research*, **37**, 189-238. https://doi.org/10.1146/annurev.matsci.37.052506.084323

[32] Horiuchi, S., Kumai, R. and Tokura, Y. (2007) A Supramolecular Ferroelectric Realized by Collective Proton Transfer. *Angewandte Chemie International Edition*, **46**, 3497-3501. https://doi.org/10.1002/anie.200700407

[33] Heredia, A., van der Strate, H.J., Delgadillo, I., Basiuk, V.A. and Vrieling, E.G. (2008) Analysis of Organo-Silica Interactions during Valve Formation in Synchronously Growing Cells of the DiatomNavicula pelliculosa. *ChemBioChem*, **9**, 573-584. https://doi.org/10.1002/cbic.200700313

[34] Heredia, A., Figueira, E., Rodrigues, C.T., Rodríguez-Galván, A., Basiuk, V.A., Vrieling, E.G. and Almeida, S.F.P. (2012) Cd2+ Affects the Growth, Hierarchical Structure and Peptide Composition of the Biosilica of the Freshwater Diatom *Nitzschia palea* (Kützing) W. Smith. *Phycological Research*, **60**, 229-240. https://doi.org/10.1111/j.1440-1835.2012.00652.x

[35] Decho, A.W. (1999) Imaging an Alginate Polymer Gel Matrix Using Atomic Force Microscopy. *Carbohydrate Research*, **315**, 330-333. https://doi.org/10.1016/S0008-6215(99)00006-3

[36] Hanwell, M.D., Curtis, D.E., Lonie, D.C., Vandermeersch, T., Zurek, E. and Hutchison, G.R. (2012) Avogadro: An Advanced Semantic Chemical Editor, Visualization, and Analysis Platform. *Journal of Cheminformatics*, **4**, 17. https://doi.org/10.1186/1758-2946-4-17

[37] Gordon, M.S. and Schmidt, M.W. (2005) Chapter 41—Advances in Electronic Structure Theory: GAMESS a Decade Later. In: Dykstra, C.E., Frenking, G., Kim, K.S. and Scuseria G.E., Eds., *Theory and Applications of Computational Chemistry*,

Elsevier, Amsterdam, 1167-1189.
https://doi.org/10.1016/B978-044451719-7/50084-6

[38] Trombold, C.D. and Israde-Alcantara, I. (2005) Paleoenvironment and Plant Cultivation on Terraces at La Quemada, Zacatecas, Mexico: The Pollen, Phytolith and Diatom Evidence. *Journal of Archaeological Science*, **32**, 341-353.
https://doi.org/10.1016/j.jas.2004.10.005

[39] Desikachary, T.V. and Dweltz, N.E. (1961) The Chemical Composition of the Diatom Frustule. *Proceedings of the Indian Academy of Science*, *Section B*, **53**, 157-165.

[40] Sarker, B., Papageorgiou, D.G., Silva, R., Zehnder, T., Gul-E-Noor, F., Bertmer, M., Kaschta, J., Chrissafis, K., Detsch, R. and Boccaccini, A.R. (2014) Fabrication of Alginate-Gelatin Crosslinked Hydrogel Microcapsules and Evaluation of the Microstructure and Physico-Chemical Properties. *Journal of Materials Chemistry B*, **2**, 1470. https://doi.org/10.1039/c3tb21509a

[41] Daemi, H. and Barikani, M. (2012) Synthesis and Characterization of Calcium Alginate Nanoparticles, Sodium Homopolymannuronate Salt and Its Calcium Nanoparticles. *Scientia Iranica*, **19**, 2023-2028.
https://doi.org/10.1016/j.scient.2012.10.005

[42] Pacheco, N., Garnica-Gonzalez, M., Gimeno, M., Bárzana, E., Trombotto, S., David, L. and Shirai, K. (2011) Structural Characterization of Chitin and Chitosan Obtained by Biological and Chemical Methods. *Biomacromolecules*, **12**, 3285-3290.
https://doi.org/10.1021/bm200750t

[43] Heredia, A., Aguilar-Franco, M., Magaña, C., Flores, C., Piña, C., Velázquez, R., Schäffer, T.E., Bucio, L. and Basiuk, V.A. (2007) Structure and Interactions of Calcite Spherulites with α-Chitin in the Brown Shrimp (*Penaeus aztecus*) Shell. *Materials Science and Engineering*: *C*, **27**, 8-13.
https://doi.org/10.1016/j.msec.2005.11.003

[44] Musić, S., Filipović-Vinceković, N. and Sekovanić, L. (2011) Precipitation of Amorphous SiO_2 Particles and Their Properties. *Brazilian Journal of Chemical Engineering*, **28**, 89-94. https://doi.org/10.1590/S0104-66322011000100011

[45] Durkin, C.A., Mock, T. and Armbrust, E.V. (2009) Chitin in Diatoms and Its Association with the Cell Wall. *Eukaryotic Cell*, **8**, 1038-1050.
https://doi.org/10.1128/EC.00079-09

[46] Chen, X., Iwamoto, M., Shi, Z., Zhang, L. and Wang, Z.L. (2015) Self-Powered Trace Memorization by Conjunction of Contact-Electrification and Ferroelectricity. *Advanced Functional Materials*, **25**, 739-747.
https://doi.org/10.1002/adfm.201403577

[47] Alexe, M. and Gruverman, A. (2013) Nanoscale Characterisation of Ferroelectric Materials: Scanning Probe Microscopy Approach. Springer Science & Business Media, Berlin.

[48] Sugita, A. and Tasaka, S. (2004) Electric-Field-Induced Chain Orientation in Poly (L-Lactic Acid). *Journal of Polymer Science Part B*: *Polymer Physics*, **42**, 4433-4439.
https://doi.org/10.1002/polb.20016

[49] Sencadas, V., Ribeiro, C., Heredia, A., Bdikin, I.K., Kholkin, A.L. and Lanceros-Mendez, S. (2012) Local Piezoelectric Activity of Single Poly(L-Lactic Acid) (PLLA) Microfibers. *Applied Physics A*, **109**, 51-55.
https://doi.org/10.1007/s00339-012-7095-z

[50] Svetličić, V., Žutić, V., Radić, T.M., Pletikapić, G., Zimmermann, A.H. and Urbani, R. (2011) Polymer Networks Produced by Marine Diatoms in the Northern Adriatic

Sea. *Marine Drugs*, **9**, 666-679. https://doi.org/10.3390/md9040666

[51] Hurd, C.L. (2000) Water Motion, Marine Macroalgal Physiology, and Production. *Journal of Phycology*, **36**, 453-472. https://doi.org/10.1046/j.1529-8817.2000.99139.x

[52] Furuya, D.C., da Costa, S.A., de Oliveira, R.C., Ferraz, H.G., Pessoa Junior, A. and da Costa, S.M. (2017) Fibers Obtained from Alginate, Chitosan and Hybrid Used in the Development of Scaffolds. *Materials Research*, **20**, 377-386.